Supporting Information for:

Mechanism of enhanced strontium uptake into calcite via an amorphous calcium carbonate (ACC) crystallisation pathway

Janice Littlewood[1], Samuel Shaw[2], Caroline L. Peacock[1], Pieter Bots[2#], Divyesh Trivedi[3] and Ian T. Burke[1]

[1] Earth Surface Science Institute, School of Earth and Environment, University of Leeds, Leeds, LS2 9JT, UK. *Corresponding Author's email: i.t.burke@leeds.ac.uk

[2] School of Earth, Atmospheric and Environmental Sciences, University of Manchester, Manchester, M13 9PL, UK.

[3] National Nuclear Laboratories, Risley, Warrington, Cheshire, WA3 6AS, UK.

[#]Present address: Department of Civil and Environmental Engineering, University of Strathclyde, Glasgow, G1 1XJ, UK

Consists of 10 pages with, 1 text section, 7 tables and 4 figures.

Table S1: Carbonate precipitation experiments performed at 0.1 mol L^{-1} solution concentration.

Experiment Description	Volume CaCl$_2$ 0.1 mol L^{-1}	Volume SrCl$_2$ 0.1 mol L^{-1}	Volume MgCl$_2$ 0.1 mol L^{-1}	Volume Na$_2$CO$_3$ 0.1 mol L^{-1}
1 % Sr	9.90 mL	0.10 mL	-	10.00 mL
1 % Sr / 10 % Mg	8.90 mL	0.10 mL	1.00 mL	10.00 mL

Table S2: Carbonate precipitation experiments performed at 0.5 mol L^{-1} solution concentration.

Experiment Description	Volume CaCl$_2$ 0.5 mol L^{-1}	Volume SrCl$_2$ 0.5 mol L^{-1}	Volume MgCl$_2$ 0.5 mol L^{-1}	Volume Na$_2$CO$_3$ 0.5 mol L^{-1}
1 % Sr	9.90 mL	0.10 mL	-	10.00 mL
1 % Sr / 10 % Mg	8.90 mL	0.10 mL	1.00 mL	10.00 mL

Table S3: Carbonate precipitation experiments performed at 2.0 mol L^{-1} solution concentration.

Experiment Description	Volume CaCl$_2$ 2.0 mol L^{-1}	Volume SrCl$_2$ 2.0 mol L^{-1}	Volume MgCl$_2$ 2.0 mol L^{-1}	Volume Na$_2$CO$_3$ 2.0 mol L^{-1}
1 % Sr	9.90 mL	0.10 mL	-	10.00 mL
1 % Sr / 10 % Mg	8.90 mL	0.10 mL	1.00 mL	10.00 mL

Table S4: Carbonate precipitation experiments performed at Sr^{2+} : Ca^{2+} ratios > 10% Sr.

Experiment Description	Volume CaCl$_2$ 1.0 mol L^{-1}	Volume SrCl$_2$ 1.0 mol L^{-1}	Volume MgCl$_2$ 1.0 mol L^{-1}	Volume Na$_2$CO$_3$ 1.0 mol L^{-1}
15 % Sr	8.50 mL	1.50 mL	-	10.00 mL
25 % Sr	7.50 mL	2.50 mL	-	10.00 mL
50 % Sr	5.00 mL	5.00 mL	-	10.00 mL
75 % Sr	2.50 mL	7.50 mL	-	10.00 mL

Section S1: X-ray absorption spectroscopy (XAS) data collection and analysis

All samples were analysed as pressed pellets (without diluent) sealed in Kapton tape in fluorescence mode (0.1 ad 1 % Sr) or transmission mode (10 % Sr) as appropriate. Samples recovered from experiments after short reaction times (seconds – minutes) were prepared at the beamline laboratories immediately before data collection, other samples prepared (as pressed pellets) from carbonate powders recovered from experiments and stored at room temperature in a desiccator prior to data collect. XAS data was also collect from a 1000 or 3000 mg L^{-1} Sr^{2+} aqueous solution.

The Sr XAS data presented in this study were gathered from two distinct beamline sessions at Beamline B18 at the Diamond Light Source and Dutch Belgian Beamline (DUBBLE) at the European Synchrotron Radiation Facility (ESRF) (full sample schedule is detailed in SI Table S5 below).

At Beamline B18 at the Diamond Light Source the incident beam has a typical operating voltage of 3GeV and a current of 300mA. The x-rays at B18 are generated from a bending magnet source. The beam is vertically collimated by a Si mirror before passing through a double crystal Si monochromator. It was then focused onto the sample to give a spot size of 200 x 250 μm. Sr K edge (16105 keV) XAS spectra were gathered from fluorescence x-rays using a 9 element Ge solid state detector. The sample was held at 80K in a liquid nitrogen cryostat during data collection to improve the signal to noise ratio.

The Dutch Belgian Beamline (DUBBLE) at the European Synchrotron Radiation Facility (ESRF) operates using an incident beam voltage of 6.04 GeV and a current of 200mA. DUBBLE uses a bending magnet source which is vertically collimated by a Si mirror. The correct beam energy is then selected using a double crystal Si monochromator. The final incident beam has a spot size of 400 x 350 μm. Again at the ESRF a 9 element Ge detector was used to gather Sr K-edge fluorescence spectra. Data collection was also performed at 80 K in a liquid nitrogen cooled cryostat.

EXAFS data analysis and fitting

Multiple XAS scans from each sample were summed and averaged using Athena v 0.8.056 [1] to maximise the signal/noise ratio and XANES data was plotted. The background subtraction of the Sr EXAFS was then performed using PySpline v1.1 [2]. The EXAFS spectra were then fitted in k-space using DLexcurv v1.0 following full curved wave theory [3]. Ab initio calculations of the phaseshifts were performed using the Hedin-Lundqvist potentials and assuming the von-Barth ground states for all atoms29. Shell-by-shell fitting was then performed by estimating initial parameters for shells of backscattering atoms and then interactively refining these parameters. Specifically fits were

determined by refining number of atoms (± 25%), interatomic distances (± 0.02 Å in the first shell and ± 0.05 Å in subsequent shells), Fermi energy and Debye-Waller factor ($2\sigma^2$, ± 25%). This procedure was performed initially with a single shell and subsequent shells of surround atoms were added. Additional shells were then accepted where they improved the overall fit quality by greater than 10% (determined by reduction of the reduced Chi-squared measure of fit).

Table S5: Samples schedule for XAS analysis.

| Experiment Description	Reaction time	Primary CaCO$_3$ phase	Beamline	Synchrotron
0.1 % Sr	<30 sec	ACC	B18	DLS
	1 min	vaterite	B18	DLS
	2 hrs	calcite	B18	DLS
	24 hrs	calcite	B18	DLS
1 % Sr	<30 sec	ACC	DUBBLE	ESRF
	1 min	vaterite	DUBBLE	ESRF
	24 hrs	calcite	B18	DLS
10 % Sr	<30 sec	ACC	DUBBLE	ESRF
	1 min	vaterite	B18	DLS
	2 hrs	calcite	B18	DLS
	24 hrs	calcite	B18	DLS
0.1 % Sr / 10 % Mg	5 min	ACC	B18	DLS
	4 hrs	calcite	B18	DLS
	24 hrs	calcite	B18	DLS
1 % Sr / 10 % Mg	5 min	ACC	B18	DLS
	24 hrs	calcite	DUBBLE	ESRF
10 % Sr / 10 % Mg	5 min	ACC	B18	DLS
	4 hrs	calcite	B18	DLS
	24 hrs	calcite	DUBBLE	ESRF
*Sr$^{2+}_{(aq)}$ 1000 mg L^{-1}	-	-	B18	DLS
Sr$^{2+}_{(aq)}$ 3000 mg L^{-1}	-	-	DUBBLE	ESRF

*aqueous sample data presented in main text.
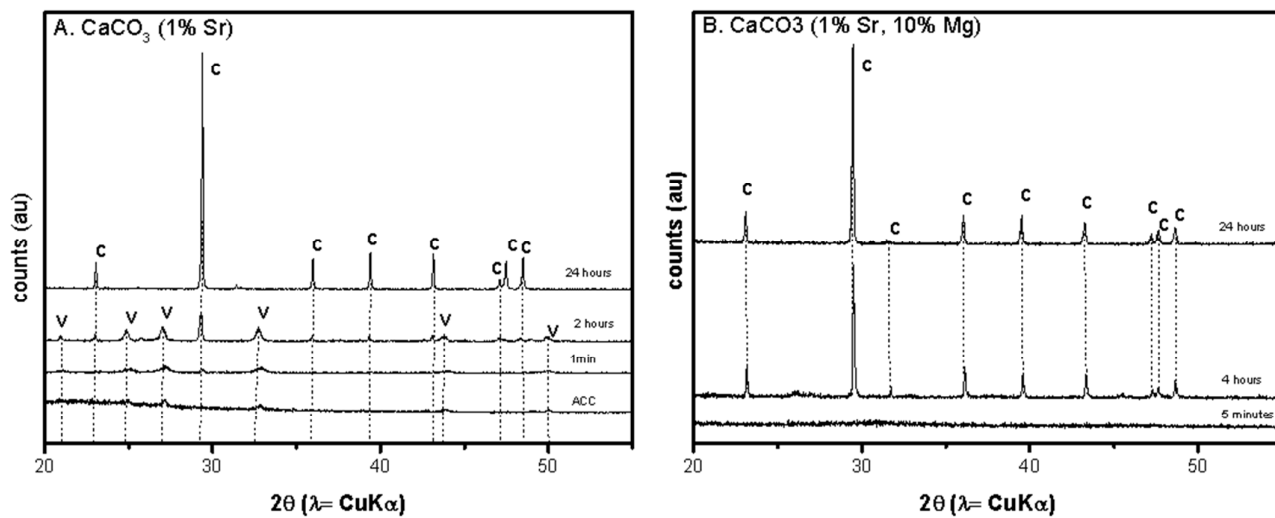
Figure S1. X-ray diffraction patterns showing the mineral phases detected during the crystallisation of CaCO3 in 1 % Sr (A) and 1 % Sr / 10 % Mg (B) experiments described in Table 1 ([Me^{2+}] = 1 mol L^{-1}). Calcite is annotated as c, vaterite is annotated as v.
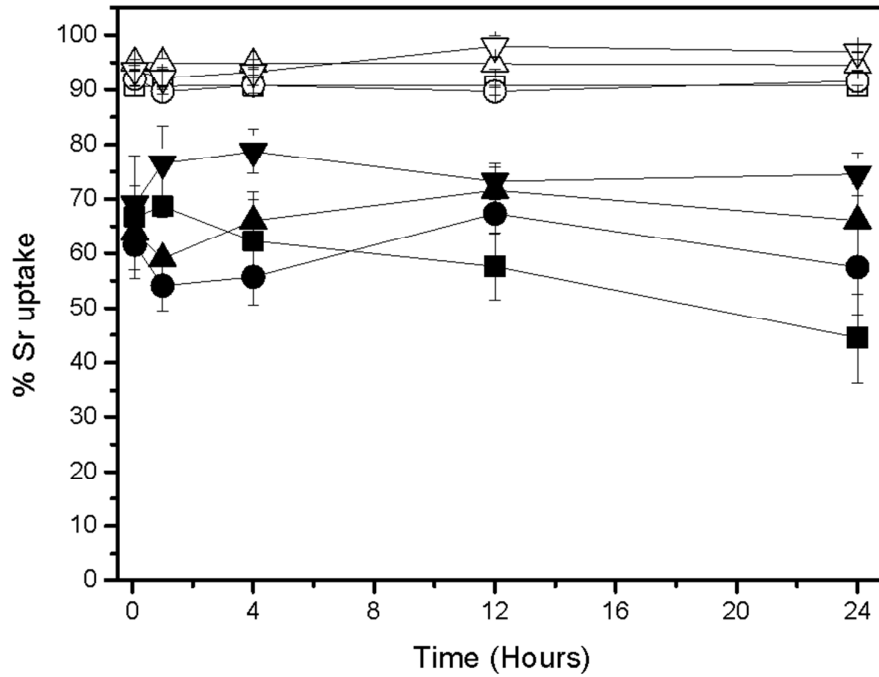
Figure S2: % [90]Sr uptake as a function of time, where 1% Sr was substituted for 1% Ca at concentrations of 0.1 M (squares), 0.5 M (circles), 1.0 M (triangle), 2.0 M (inverted triangle) and % [90]Sr uptake as a function of time, where 1% Sr/10%Mg was substituted for Ca (corresponding open symbols)
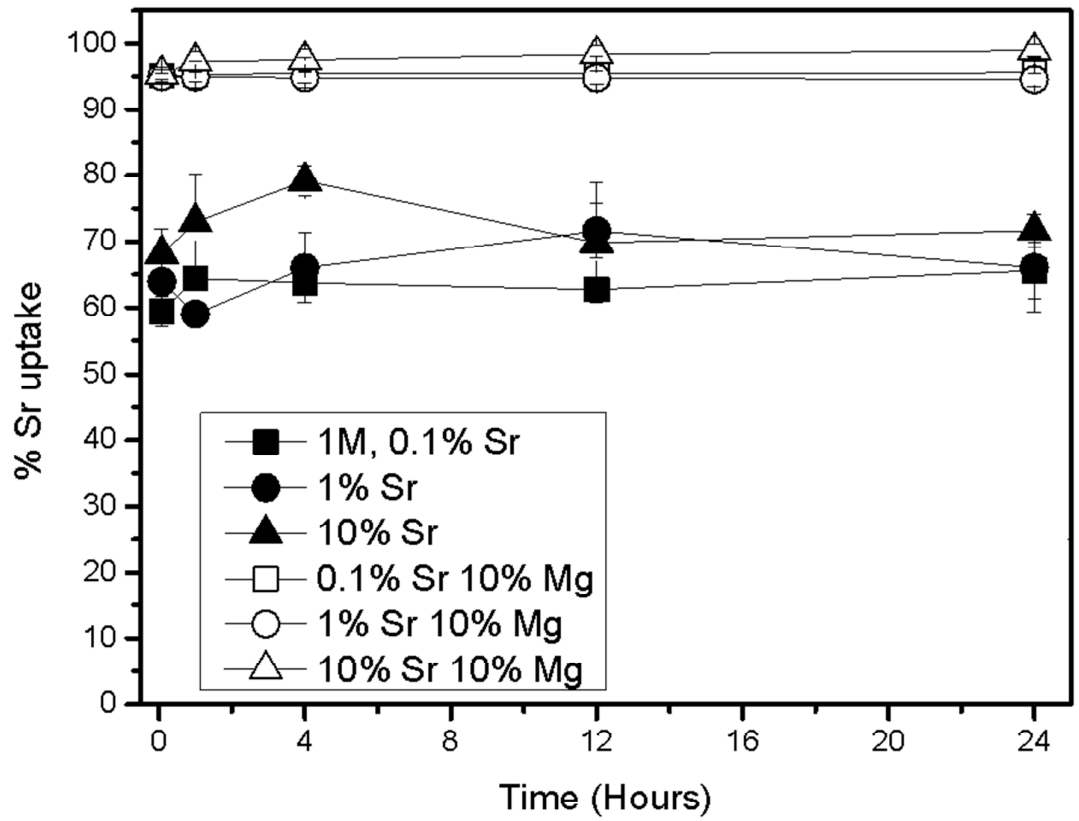
Figure S3: % [90]Sr uptake as a function of time, where Sr was substituted for Ca in the 1M starting solutions. 0.1% Sr substitution (squares), 1% Sr (circles), 10% Sr (triangle), 0.1% Sr/10% Mg (corresponding open symbols)

Table S6 Selected fits for Sr and Ca K-edge EXAFS data reported from literature.

Description	Shell	N	R (Å)	Reference
$Ca^{2+}_{(aq)}$	O	8	2.43	[4]
Ca-ACC	O	7.6	2.43	[5]
Sr-Ca-Si-H	O	6-8	2.60	[6]
Sr-calcite	O	6	2.50	[7]
	C	3	3.32	
	Ca	6	4.10	
	O	6	2.51	[8]
	C	6	3.33	
	Ca	6	4.07	
	Ca	6	5.00	
Sr-aragonite	O	9	2.58	[9]
	C	6	2.98	
	Ca	6	4.02	
Sr-vaterite	O	8	2.55	[8]
	C	6	2.94	
	Ca	4	4.17	
$SrCO_3$	O	9	2.60	[7]
	C	3	3.05	
	C	3	3.41	
	Sr	6	4.16	
	Sr	6	4.91	
	O	9	2.60	[10]
	C	6	3.05	
	Sr	6	4.22	
	Sr	4	4.97	
	O	9	2.61	[11]
	C	4	3.04	
	Sr	4	4.14	
	Sr	2	4.29	
	Sr	4	4.90	

Table S7: Average trace element uptake (mol%) determined in calcite end products from crystallisation experiments. [Me^{2+}] = 1 mol L^{-1}. % Sr uptake was determined from % ^{90}Sr uptake in experiments, Mg uptake was determined by ICP-MS analysis of the solid calcite product after dissolution in nitric acid (10 mg calcite dissolved in 10 ml 0.1 M HNO$_3$).

Experiment Description	Sr (mol% SrCO3)	Mg (mol% MgCO$_3$)
0.1 % Sr	0.07 ±0.01	-
1 % Sr	0.66±0.07	-
10 % Sr	6.80 ±0.43	-
0.1 % Sr / 10 % Mg	0.14 ±0.01	4.14 ±0.12
1 % Sr / 10 % Mg	1.12 ±0.03	4.31 ±0.13
10 % Sr / 10 % Mg	10.27 ±0.30	5.70 ±0.17
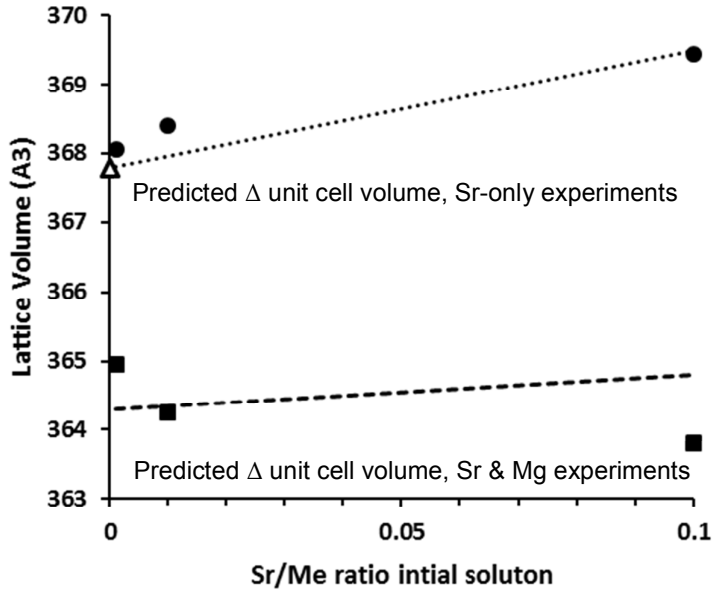
Figure S4. Predicted effect of increasing Sr^{2+} and Mg^{2+} uptake on measured unit cell volume in Mg-free and high-Mg experiments. Dotted line indicate the trend in unit cell volume expected for the measured change in mol % Sr and mol % Mg content shown in Table S7 & unit cell volume data from [12]. Dashed line indicates the predicted change in unit cell volume expected from a simple linear combination of the separate Sr^{2+} + Mg^{2+} effects using data from Table S7 and [12, 13]. Open triangle is unit cell volume of pure calcite ($CaCO_3$).

SI REFERENCES

[1] B. Ravel, M. Newville, ATHENA, ARTEMIS, HEPHAESTUS: data analysis for X-ray absorption spectroscopy using IFEFFIT, Journal of synchrotron radiation, 12 (2005) 537-541.

[2] A. Tenderholt, B. Hedman, K.O. Hodgson, PySpline: a modern, cross-platform program for the processing of raw averaged XAS edge and EXAFS data, X-Ray Absorption Fine Structure--XAFS 13, 882 (2007) 105-107.

[3] S. Tomic, B. Searle, A. Wander, N. Harrison, A. Dent, J. Mosselmans, J. Inglesfield, New tools for the analysis of EXAFS: the DL EXCURV package, Council for the Central Laboratory of the Research Councils, (2005).

[4] F. Jalilehvand, D. Spångberg, P. Lindqvist-Reis, K. Hermansson, I. Persson, M. Sandström, Hydration of the Calcium Ion. An EXAFS, Large-Angle X-ray Scattering, and Molecular Dynamics Simulation Study, Journal of the American Chemical Society, 123 (2001) 431-441.

[5] Y. Politi, Y. Levi-Kalisman, S. Raz, F. Wilt, L. Addadi, S. Weiner, I. Sagi, Structural characterization of the transient amorphous calcium carbonate precursor phase in sea urchin embryos, Advanced Functional Materials, 16 (2006) 1289-1298.

[6] E. Wieland, J. Tits, D. Kunz, R. Dähn, Strontium uptake by cementitious materials, Environmental Science and Technology, 42 (2008) 403-409.

[7] R.H. Parkman, J.M. Charnock, F.R. Livens, D.J. Vaughan, A study of the interaction of strontium ions in aqueous solution with the surfaces of calcite and kaolinite, Geochimica et Cosmochimica Acta, 62 (1998) 1481-1492.

[8] L. Brinza, P.D. Quinn, P.F. Schofield, J.F.W. Mosselmans, M.E. Hodson, Incorporation of strontium in earthworm-secreted calcium carbonate granules produced in strontium-amended and strontium-bearing soil, Geochimica et Cosmochimica Acta, 113 (2013) 21-37.

[9] A.A. Finch, N. Allison, S.R. Sutton, M. Newville, Strontium in coral aragonite: 1. Characterization of Sr coordination by extended absorption X-ray fine structure, Geochimica et Cosmochimica Acta, 67 (2003) 1197-1202.

[10] S.H. Wallace, S. Shaw, K. Morris, J.S. Small, I.T. Burke, Alteration of sediments by hyperalkaline K-rich cement leachate: implications for strontium adsorption and incorporation, Environmental science & technology, 47 (2013) 3694-3700.

[11] P.A. O'Day, M. Newville, P.S. Neuhoff, N. Sahai, S.A. Carroll, X-ray absorption spectroscopy of strontium(II) coordination. I. Static and thermal disorder in crystalline, hydrated, and precipitated solids and in aqueous solution, Journal of Colloid and Interface Science, 222 (2000) 184-197.

[12] S. Matsunuma, H. Kagi, K. Komatsu, K. Maruyama, T. Yoshino, Doping Incompatible Elements into Calcite through Amorphous Calcium Carbonate, Crystal Growth & Design, 14 (2014) 5344-5348.

[13] W.D. Bischoff, F.C. Bishop, F.T. Mackenzie, Biogenically produced magnesian calcite; inhomogeneities in chemical and physical properties; comparison with synthetic phases, American Mineralogist, 68 (1983) 1183-1188.